光学学报

光学焦散线的任意无衍射结构光场调控

兰燕平[1]，胡俊涛[1]，孙卓[1]，王逸舒[1]，叶文妮[1]，钱义先[1,2*]

[1]浙江师范大学物理与电子信息工程学院，浙江 金华 321004；
[2]浙江省光信息检测与显示技术重点实验室，浙江 金华 321004

摘要 从几何光学焦散角度，利用谱相位调制原理，提出一种通用且高效的无衍射结构光场调控方法。利用驻相近似和焦散线原理建立了谱相位与光束横截面分布轨迹之间的数学模型。提出一种谱相位叠加的改进算法，实现构建任意结构的无衍射光束，理论模拟和实验结果相吻合。与现有方法相比，本文方法能够实现对无衍射光场形状分布的灵活调控，其丰富的结构及无衍射特性将极大地拓展其在光学微加工及微操纵等领域的应用。

关键词 物理光学；无衍射光束；光学焦散线；相位调制

中图分类号 O436　　**文献标志码** A　　　　　　　　　　**DOI：** 10.3788/AOS230433

1 引　　言

近年来，新型结构光束如无衍射光束[1-3]、自加速光束[4-6]、涡旋光束[7-8]、矢量光束[9-11]等引起研究人员广泛关注，这些新颖光束展现了一系列新颖的物理效应，如无衍射、自弯曲传输、光子轨道角动量以及超衍射极限紧聚焦等光学特性。其中，无衍射光束能够在传播过程中使光强分布保持不变，在激光微加工[12-14]、微粒操纵[15-17]以及显微成像[18-21]等领域具有广泛的应用。

最早的无衍射光束是 1987 年 Durnin[22]发现的贝塞尔光束，该光束是从柱坐标系下的亥姆霍兹方程求得的一个具有贝塞尔函数形式的波包解。在传播方向的演化中，该特殊解具有光强分布不变、能量高度局域化的特点。随后，余弦光束[23]、马蒂厄光束[24]、韦伯光束[25-26]等无衍射光束分别从直角坐标系、椭圆坐标系以及抛物线坐标系下的波动方程求解得到。随后，更多具有无衍射特性的光束也分别通过这些基本无衍射光束进行叠加产生[27-30]。此外，最近发现的艾里光束，除了具有无衍射特性外，还表现出独特的自加速、自愈等奇异特性[4-5]。这些光束丰富了无衍射光束家族。

上述无衍射光束最初都是在不同的坐标系下，通过求解波动微分方程或亥姆霍兹方程产生的。然而，通过解偏微分方程获得更多这种无衍射解析解并不容易，而且这类偏微分方程的无衍射解析解十分稀少。因此，无衍射光场结构总是局限于简单的几种形式，其应用也受到极大的限制。本文基于几何光学焦散线原理[31-32]，提出了一种简洁、通用的方法来产生任意结构的无衍射光束，推导并建立无衍射光束分布轨迹与其谱相位的数学模型，并提出一种改进算法，通过分割光场分布的轨迹曲线，利用相位叠加原理，实现任意结构无衍射光场的定制，产生的目标光束将极大地拓展其在光学微加工和微操纵中的应用。

2 原　　理

无衍射光场 $\phi(x,y,z)$ 可以用 Whittaker 积分[24]表示为

$$\phi(x,y,z) = \exp(\mathrm{i}k_z z)\int A(\varphi)\exp\big[\mathrm{i}k_t(x\cos\varphi + y\sin\varphi)\big]\mathrm{d}\varphi, \tag{1}$$

式中：$A(\varphi)$ 为角谱，φ 为方位角；z 为传播方向；$k_z = k\cos\vartheta$ 为轴向波矢分量，下标 z 为该轴向波矢分量与传播方向 z 轴对应，ϑ 为任意一个角度常数；k_t 为横向波矢分量，$k_t = \sqrt{k_x^2 + k_y^2} = k\sin\vartheta$，因此 $k = \sqrt{k_z^2 + k_t^2}$；$\exp(\mathrm{i}k_z z)$ 是与积分变量 φ 无关的函数，在求光强时最终因共轭而消去，后续推导时省略。引言提及的 4 种无衍射光束分别是在笛卡儿坐标、圆柱坐标、圆柱椭圆坐标、圆柱抛物线坐标系及可分离变量情况下，通过求解二维亥姆霍兹方程获得。这样的无衍射解十分稀少，造成无衍射光场结构十分有限。式（1）中，由于角谱 $A(\varphi)$ 可以是任意函数，意味着存在无限多种结构的无衍射光束，因为光场角谱完全定义了光束特性。式（1）可以理解为波面位于圆心角为 ϑ 的锥面上的平

面波叠加,即这些平面光的波矢具有相同的倾角 ϑ,在傅里叶空间中呈现为圆锥结构,如图 1 所示。当角谱 $A(\varphi)$ 发生改变时,可以获得具有预定义结构的无衍射光场。
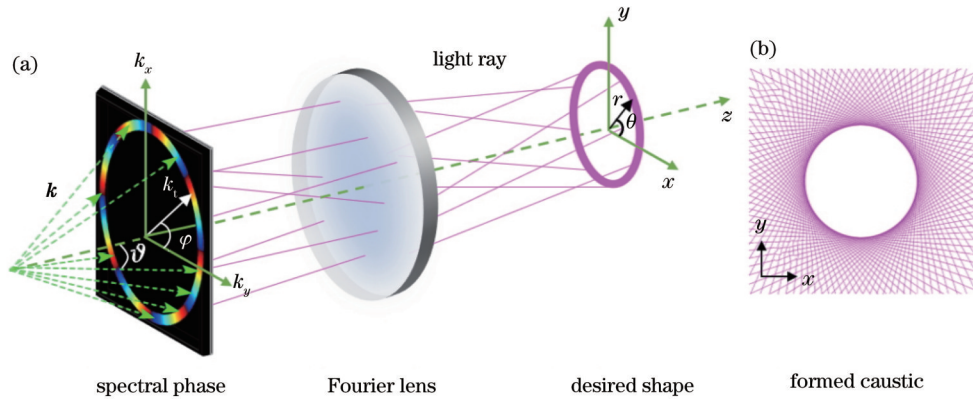

图 1 谱相位调制产生无衍射光束示意图。(a)谱相位调制方法;(b)具有特定形状分布的焦散线

Fig. 1 Schematic diagram of generating non-diffracting beams via spectral phase modulation. (a) Spectral phase modulation; (b) caustics with specific structure

为了实现任意结构的无衍射光场定制,从几何光学焦散线的视角,建立谱相位与光场的横向分布轨迹曲线的数学模型。首先,将复函数角谱表示为 $A(\varphi)=g(\varphi)\exp[\mathrm{i}\varPhi(\varphi)]$,其中,$g(\varphi)$ 为振幅,$\varPhi(\varphi)$ 为相位,代入式(1),可得初始光场表达式为

$$\phi(x,y)=\int_0^{2\pi}g(\varphi)\exp\left\{\mathrm{i}\left[\varPhi(\varphi)+k_{\mathrm{t}}\left(x\cos\varphi+y\sin\varphi\right)\right]\right\}\mathrm{d}\varphi。 \quad(2)$$

式(2)可通过驻相近似法化简并求解。驻相近似法的原理为将衍射积分的主要贡献看成来源于谱相位面上的驻相点附近的相位,其他位置的相位点贡献可相互抵消。因此,在驻相点附近的位置上,积分式中的相位部分满足一阶导数为零,即

$$\varPhi'(\varphi)+k_{\mathrm{t}}(-x\sin\varphi+y\cos\varphi)=0, \quad(3)$$

式中:$\varPhi'(\varphi)$ 为 φ 的一阶导数。在给定的方位角 φ 下,该式为关于 x 和 y 的线性方程,从几何光学的角度来看,该线性方程描述了一条从相位平面上的一点发出的几何光线;这意味着几何光学里每一个频率 k_{t} 定义唯一一条从相位平面发出的光线,如图 1 所示。假设无衍射光束的光场结构用轨迹 $f(\theta)=(x,y)$ 描述,其中,θ 为 (x,y) 对应的方位角,且 $x=r(\theta)\cos\theta$,$y=r(\theta)\sin\theta$,如图 1 所示。然后,对式(3)关于 x 求一阶求导:

$$\frac{\mathrm{d}y}{\mathrm{d}x}=\tan\varphi, \quad(4)$$

式中:$\mathrm{d}y/\mathrm{d}x$ 为轨迹 $f(\theta)=(x,y)$ 的切线。因此,式(3)进一步表明从相位平面上发出的每一条光线都与曲线 $f(\theta)=(x,y)$ 相切。因此,光场可以看成是由相位面发出(经过透镜)的光线簇的包络面所形成的,如图 1 所示。从几何光学的角度来看,这些光线簇形成的包络面称为焦散,特指光线最集中的区域。

x 与 y 是方位角 θ 的函数,根据式(4)可以导出:

$$\varphi(\theta)=\arctan\frac{r'(\theta)\sin\theta+r(\theta)\cos\theta}{r'(\theta)\cos\theta-r(\theta)\sin\theta}。 \quad(5)$$

为了让无衍射光束具有光强极大值,对式(3)关于 φ 求二阶导数 $\varPhi''(\varphi)$,并满足二阶导数为 0:

$$\varPhi''(\varphi)=k_{\mathrm{t}}(x\cos\varphi+y\sin\varphi)。 \quad(6)$$

联立式(3)、式(5)、式(6),可推导出描述无衍射结构光的横截面光场分布曲线 $f(\theta)=(x,y)$ 所对应的相位表达式为

$$\varPhi(\varphi)=-k_{\mathrm{t}}\int\left[-x\theta(\varphi)\sin\varphi+y\theta(\varphi)\cos\varphi\right]\mathrm{d}\varphi, \quad(7)$$

式中:$\theta(\varphi)$ 为 $\varphi(\theta)$ 的反函数。式(7)描述了横向光场分布形状 $f(\theta)$ 和谱相位 $\varPhi(\varphi)$ 的一一对应数学模型,通过提前设定光场的分布曲线,可以获得对应的相位分布,进而产生所需的无衍射结构光场。因此,该方法打破了传统的解偏微分方程获得无衍射解的束缚,极大丰富无衍射光场家族。

3 数值模拟

以贝塞尔光束为例,其光场形状轨迹为圆形,令其表达式为 $x^2+y^2=r_0^2$,其中 r_0 为圆的半径,可以取值为任意大于 0 的常数,该表达式的参数形式为 $x=r_0\cos\theta$,$y_0=r_0\sin\theta$,由式(5)可得,$\varphi=\arctan(1/\tan\theta)$,将该结果代入式(7),计算得到该光场形状对应的谱相位表达式为 $\varPhi(\varphi)=k_{\mathrm{t}}r_0\varphi$,根据式(2)可得到该无衍射光束的解析表达式为 $\phi(r,\theta,z)=\mathrm{J}_m(k_{\mathrm{t}}r)\exp(\mathrm{i}k_zz-\mathrm{i}m\theta)$,其中,$m=k_{\mathrm{t}}r_0$,$\mathrm{J}_m$ 为第一类 m 阶贝塞尔函数,该式正好与贝塞尔光束的解析解吻合[22]。

图 2(a1)~(a3)为光场形状为圆形的贝塞尔光束,其中 $r_0=30/k_{\mathrm{t}}$。图 2(a1)为贝塞尔光束的环形谱相位,图 2(a2)为 x-y 平面的焦散线示意图,图 2(a3)为贝塞尔光束的初始光场。所有数值模拟中,如无特殊说

明，$\lambda = 632.8$ nm，$k_t = 16.75$，振幅 $g(\varphi) = 1$。模拟结果中的实空间坐标 $x = X/x_0$、$y = Y/y_0$、$z = Z/z_0$ 都为无量纲，且比例因子分别为 $x_0 = y_0 = 0.35$ mm、$z_0 = 1$ mm。
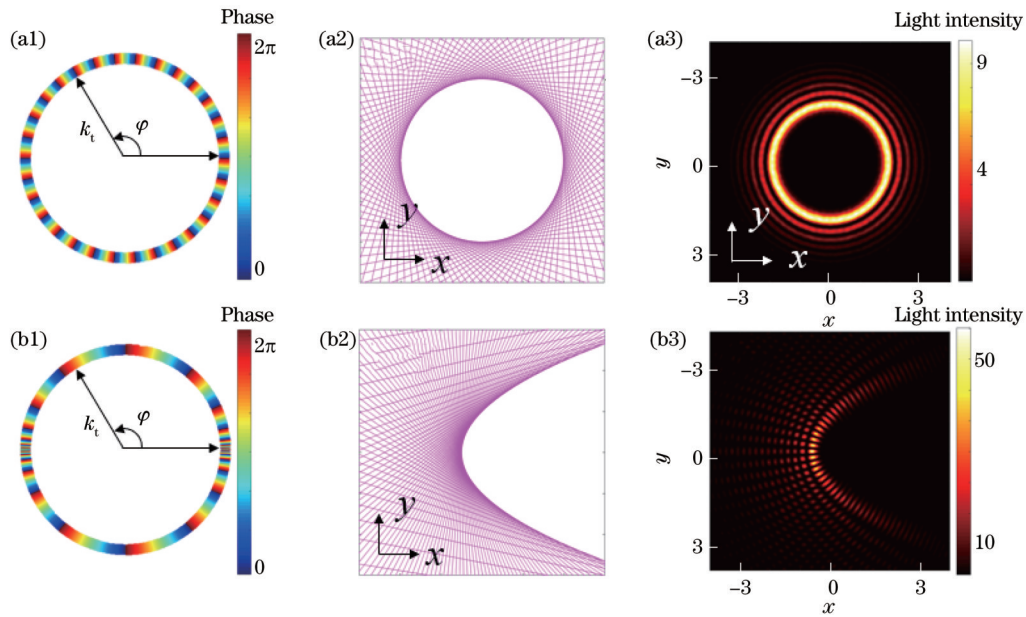

图 2　不同形状分布的无衍射光束。(a1)贝塞尔光束的谱相位；(a2)贝塞尔光束的焦散线；(a3)贝塞尔光束的横向初始光场分布图；(b1)抛物线 Webber 无衍射光束的谱相位；(b2)抛物线 Webber 无衍射光束的焦散线；(b3)抛物线 Webber 无衍射光束的横向初始光场分布图

Fig. 2　Non-diffracting beams with varied structures. (a1) Spectral phase for non-diffracting Bessel beam; (a2) caustics for non-diffracting Bessel beam; (a3) initial intensity distribution for non-diffracting Bessel beam; (b1) spectral phase for non-diffracting Webber beam; (b2) caustics for non-diffracting Webber beam; (b3) initial intensity distribution for non-diffracting Webber beam

图 2(b1)~(b3)为抛物线 Webber 无衍射光束，其光场形状轨迹曲线的参数方程为 $x = 2a\cos\theta/(1-\cos\theta)$，$y = 2a\sin\theta/(1-\cos\theta)$，其中，$a = 0.5$，该轨迹对应的谱相位表达为 $\Phi(\varphi) = ak_t\ln\left[\tan(\varphi/2)\right]$，对应谱相位结构如图 2(b1)所示。图 2(b2)、(b3)分别为无衍射 Webber 光束的焦散线示意图和初始光场分布。由图 2 可知，其横截面光场分布吻合预设的轨迹。

由式(5)可知，θ 和 φ 具有一一对应的关系，即从谱相位面上任何一点发出的光线，都与光场分布曲线相切，因此 $\varphi(\theta)$ 具有单调性，这意味着由式(7)建立的数学关系式只适合凸或凹轨迹的形状曲线。为了产生更加复杂、包含凹凸轨迹的任何形状的曲线，提出一种改进的算法，将复杂轨迹在曲线拐点处分割，分成多个子轨迹，实现每个子轨迹均满足式(7)，如图 3 所示。然后基于复振幅叠加的方法，推导出更为通用的谱相位和光场分布曲线的数学模型。每个子轨迹对应的谱相位可以通过式(7)计算，因此叠加相位 $\Phi_t(\varphi)$ 表达式为

$$\Phi_t(\varphi) = \sum_{j=1}^{N}\Phi_j(\varphi), \varphi \in \left[\varphi_{j1}, \varphi_{j2}\right], \quad (8)$$

式中：$\Phi_j(\varphi)$ 为第 j 个子复振幅的谱相位；φ_{j1}、φ_{j2} 分别为第 j 个角谱方位角的上下限，满足 $-\pi \leqslant \varphi_{j1} < \varphi_{j2} \leqslant \pi$。通过式(8)可以实现任意结构无衍射光束的定制。

对结构更为复杂的无衍射光束进行分析，以肾型

和 8 字型为例，分别模拟这两种结构的无衍射光束的结果，如图 3 所示。对肾型结构光束而言，其曲线的参数表达式为 $\begin{cases} x = a\left[3\cos\theta - \cos(3\theta)\right] \\ y = a\left[3\sin\theta - \sin(3\theta)\right] \end{cases}$，其中 $a = 1$。由图 3(a1)可知，其光场形状轨迹可以分为两部分，通过式(7)计算得到上、下半部分对应的谱相位分别为 $\Phi_1(\varphi) = -16ak_t\cos(\varphi - \pi/4)^2$ 和 $\Phi_2(\varphi) = -16ak_t \times \cos(\varphi + \pi/4)^2$。肾型无衍射光束的轨迹分割示意图、初始光场分布、初始相位分布如图 3(a1)~(a3)所示。8 字型结构光束的轨迹分割示意图、初始光强分布、初始相位图分别如图 3(b1)~(b3)所示。可见，通过改进的算法可以产生任意结构的无衍射光束，这些丰富的无衍射结构光有望在粒子操纵等应用中展现出更多优势，将极大拓展无衍射光场在光学微加工及微操纵方面的应用潜力。

4　实验验证

实验装置如图 4 所示，氦氖激光器发出波长为 632.8 nm 的激光光束，经过空间滤波器扩束准直后，垂直入射到纯相位液晶空间光调制器（分辨率为 1920 pixel×1080 pixel，像元大小为 8 μm，型号为 Holoeye）上，该空间光调制器预先加载了计算得到的谱相位。经过该相位的调制后的光束最终在透镜($f=$
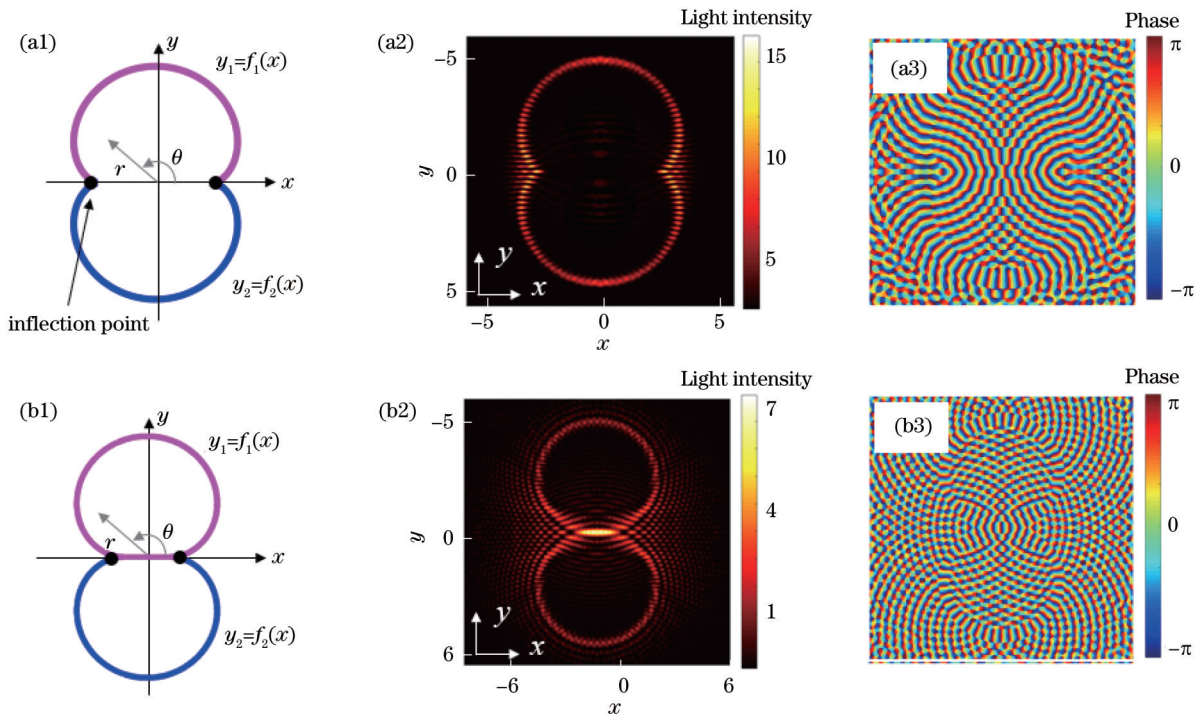
图 3　任意结构的无衍射光束。(a1)肾型无衍射光束的曲线分割；(a2)肾型无衍射光束的初始光场分布；(a3)肾型无衍射光束的初始相位图；(b1)8字型无衍射光束的曲线分割；(b2)8字型无衍射光束的初始光场分布；(b3)8字型无衍射光束的初始相位图

Fig. 3　Non-diffracting beams with arbitrary structures. (a1) Segmental graph of kidney-shaped non-diffracting beam; (a2) initial intensity distribution of kidney-shaped non-diffracting beam; (a3) phase pattern of kidney-shaped non-diffracting beam; (b1) segmental graph of 8-shaped non-diffracting beam; (b2) initial intensity distribution of 8-shaped non-diffracting beam; (b3) phase pattern of 8-shaped non-diffracting beam

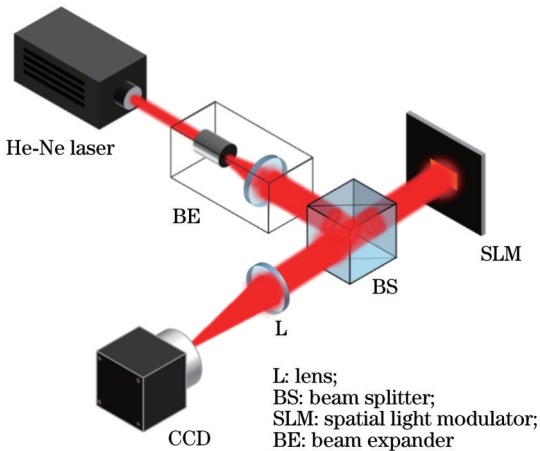300 mm）的后焦面产生所需无衍射光束，其光强分布由可移动的 CCD 记录。

图 4　实验装置图
Fig. 4　Experimental setup

　　实验上以产生心型无衍射光束为例，其光场轨迹的参数方程为 $x = 2a\cos\theta - a\cos(2\theta)$，$y = 2a\sin\theta - a\sin(2\theta)$，其中，$a = 1$。通过式（7）计算得到的谱相位示意图如图 5(a)所示。该光束的传播演化结果如图 5(b)所示。该光束能够在很长一段距离内保持光强分布不变特性。图 5(c1)～(c3)分别为该光束在 $z =$

0、60、100 位置的光场分布图。图 5(d1)～(d3)为 $Z = $ 0、60、100 mm 位置的实验结果。由图 5 可知，模拟结果与实验结果较好吻合，光场分布与预设吻合，且在较长的传播距离内光场保持不变，呈现明显的无衍射特性。

　　为了实验证实可以产生更复杂的无衍射结构光，图 6(a1)～(a3)为 8 字型结构的无衍射光束在 $z = 0$、60、100 位置的模拟光场分布，图 6(b1)～(b3)为 $Z = 0$、60、100 mm 位置的实验结果。显然，对复杂结构的模拟结果和实验结果依然较好吻合，对任何复杂结构的无衍射光场，所提算法都能展现出很好的稳健性。因此，通过改进的算法可以产生任意结构的无衍射光束，其将极大拓展无衍射光场在光学微加工及微操纵方面的应用潜力。

5　结　　论

　　所提方法能构建横截面上具有任意结构分布的无衍射光场，该方法简洁、通用、高效，打破了传统方法中通过求解不同坐标系下亥姆霍兹偏微分方程，获得无衍射光场的限制，能够按照需求实现任意无衍射结构光束的定制，产生各种各样的无衍射结构光场，极大丰富无衍射光束家族，这为灵活的光学微加工、光学微操纵及波前调控，开辟了新方法，提供了一条新途径。
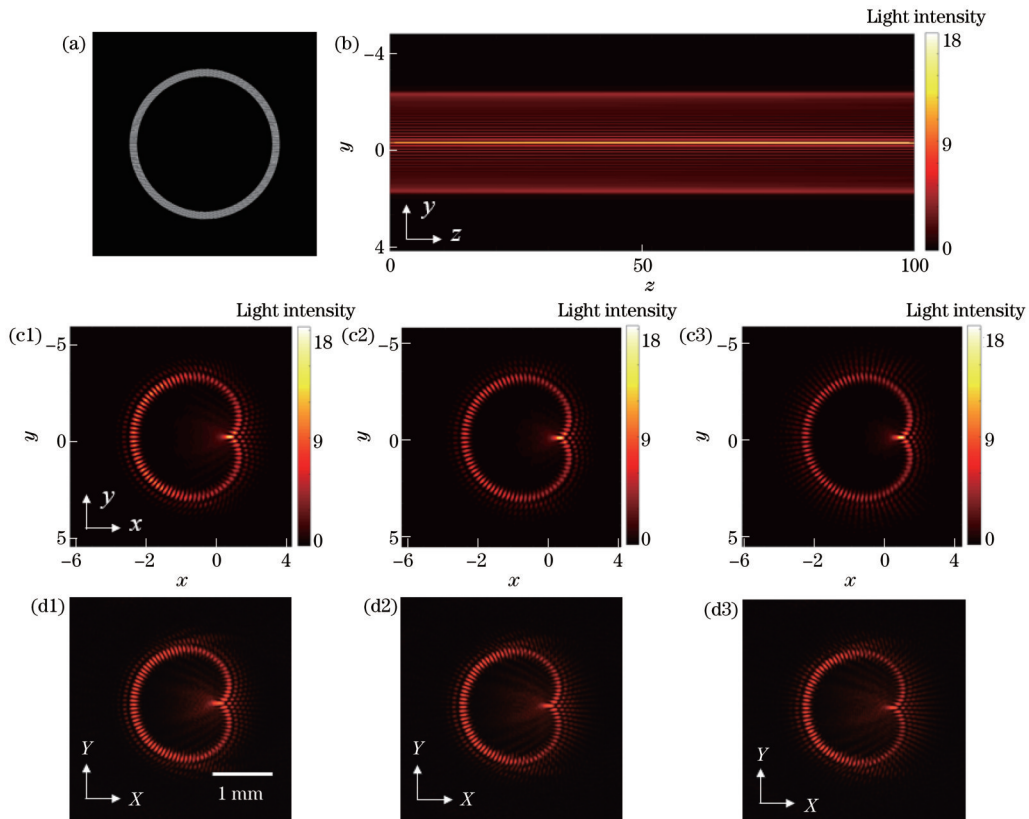
图 5 心型无衍射光束。(a)谱相位;(b)侧视演化图;(c1) $z=0$ 位置的模拟光场强度;(c2) $z=60$ 位置的模拟光场强度;(c3) $z=100$ 位置的模拟光场强度;(d1) $Z=0$ mm 位置的实验光场强度;(d2) $Z=60$ mm 位置的实验光场强度;(d3) $Z=100$ mm 位置的实验光场强度

Fig. 5 Heart-shaped non-diffracting beams. (a) Spectral phase; (b) numerical side-view; (c1) numerical intensity distribution at the propagation distance of $z=0$; (c2) numerical intensity distribution at the propagation distance of $z=60$; (c3) numerical intensity distribution at the propagation distance of $z=100$; (d1) experimental intensity distribution at the propagation distance of $Z=0$ mm; (d2) experimental intensity distribution at the propagation distance of $Z=60$ mm; (d3) experimental intensity distribution at the propagation distance of $Z=100$ mm

图 6 8字形无衍射光束。(a1) $z=0$ 位置的模拟强度分布;(a2) $z=60$ 位置的模拟强度分布;(a3) $z=100$ 位置的模拟强度分布;(b1) $Z=0$ mm 位置的实验强度分布;(b2) $Z=60$ mm 位置的实验强度分布;(b3) $Z=100$ mm 位置的实验强度分布

Fig. 6 8-shaped non-diffracting beams. (a1) Numerical intensity distribution at the propagation distance of $z=0$; (a2) numerical intensity distribution at the propagation distance of $z=60$; (a3) numerical intensity distribution at the propagation distance of $z=100$; (b1) experimental intensity distribution at the propagation distance of $Z=0$ mm; (b2) experimental intensity distribution at the propagation distance of $Z=60$ mm; (b3) experimental intensity distribution at the propagation distance of $Z=100$ mm
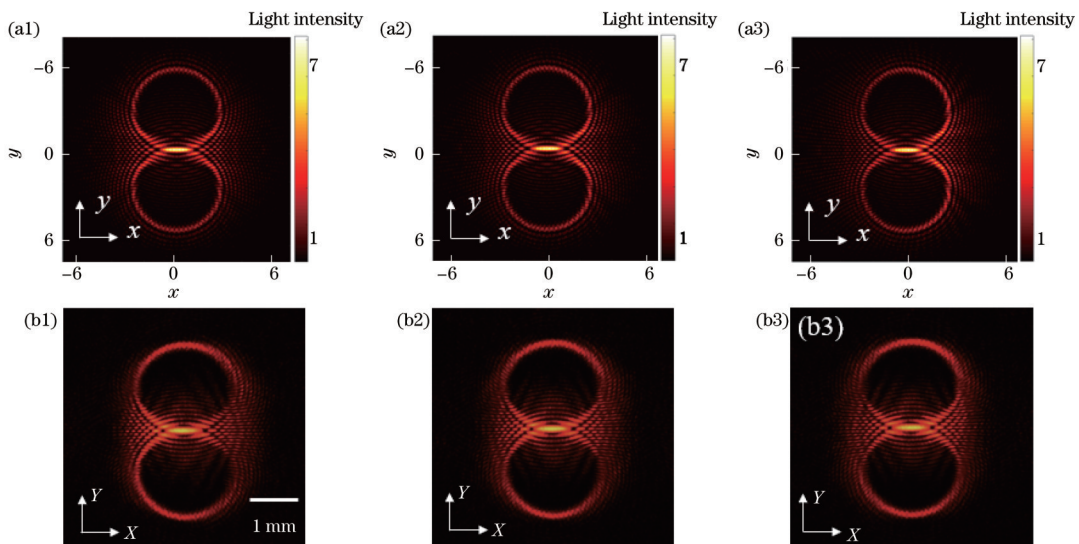
参 考 文 献

[1] Zamboni-Rached M. Carving beams of light[J]. Optics Letters，2021，46(6): 1205-1208.

[2] 谢家俊，唐诗瑶，陈永强，等. 贝塞尔光束在生物组织中的自重建特性研究[J]. 中国激光，2022，49(5): 0507302.
Xie J J, Tang S Y, Chen Y Q, et al. Self-reconstruction characteristics of Bessel beam in biological tissue[J]. Chinese Journal of Lasers，2022，49(5): 0507302.

[3] Maharjan R, Bohora S, Bhattarai P, et al. Non-diffracting beam generated from a photonic integrated circuit based axicon-like lens[J]. Optics Express，2021，29(7): 10480-10490.

[4] Greenfield E, Segev M, Walasik W, et al. Accelerating light beams along arbitrary convex trajectories[J]. Physical Review Letters，2011，106(21): 213902.

[5] Siviloglou G A, Broky J, Dogariu A, et al. Observation of accelerating airy beams[J]. Physical Review Letters，2007，99(21): 213901.

[6] 闻远辉，陈钰杰，余思远. 基于焦散线方法的自加速光束设计[J]. 物理学报，2017，66(14): 144210.
Wen Y H, Chen Y J, Yu S Y. Design of accelerating beams based on caustic method[J]. Acta Physica Sinica，2017，66(14): 144210.

[7] Li P, Zhang Y, Liu S, et al. Generation of perfect vectorial vortex beams[J]. Optics Letters，2016，41(10): 2205-2208.

[8] Zhu Y, Zhou Y W, Fan Z Y, et al. Terahertz near-field vortex beams with variable intensity profiles based on geometric metasurfaces[J]. Advanced Photonics Research，2022，3(12): 2200151.

[9] Weng X Y, Miao Y, Zhang Q L, et al. Extraction of inherent polarization modes from an m-order vector vortex beam[J]. Advanced Photonics Research，2022，3(8): 2100194.

[10] Chang C L, Gao Y, Xia J P, et al. Shaping of optical vector beams in three dimensions[J]. Optics Letters，2017，42(19): 3884-3887.

[11] 陈建，詹其文. 矢量光场与激光焦场定制[J]. 光学学报，2019，39(1): 0126002.
Chen J, Zhan Q W. Tailoring laser focal fields with vectorial optical fields[J]. Acta Optica Sinica，2019，39(1): 0126002.

[12] Nacius E, Gotovski P, Ulčinas O, et al. Spatially displaced and superposed Bessel beams for transparent material laser microprocessing[J]. Journal of the Optical Society of America B，2021，38(12): 3886-3895.

[13] Baltrukonis J, Ulčinas O, Orlov S, et al. High-order vector Bessel-Gauss beams for laser micromachining of transparent materials[J]. Physical Review Applied，2021，16(3): 034001.

[14] Duocastella M, Arnold C B. Bessel and annular beams for materials processing[J]. Laser & Photonics Reviews，2012，6(5): 607-621.

[15] An S, Peng T, Yan S H, et al. Direct axial plane imaging of particle manipulation with nondiffracting Bessel beams[J]. Applied Optics，2021，60(11): 2974-2980.

[16] Tao S H, Lee W M, Yuan X C. Dynamic optical manipulation with a higher-order fractional Bessel beam generated from a spatial light modulator[J]. Optics Letters，2003，28(20): 1867-1869.

[17] Rui G H, Wang X Y, Cui Y P. Manipulation of metallic nanoparticle with evanescent vortex Bessel beam[J]. Optics Express，2015，23(20): 25707-25716.

[18] Ali Z, Zakian C, Ntziachristos V. Elongated focus optoacoustic microscopy with matched Bessel beam illumination and ultrabroadband axicon detection[J]. Advanced Photonics Research，2022，3(5): 2100249.

[19] Nylk J, McCluskey K, Preciado M A, et al. Light-sheet microscopy with attenuation-compensated propagation-invariant beams[J]. Science Advances，2018，4(4): eaar4817.

[20] Nagar H, Dekel E, Kasimov D, et al. Non-diffracting beams for label-free imaging through turbid media[J]. Optics Letters，2018，43(2): 190-193.

[21] 陈雪利，王鑫宇，闫天宇，等. 贝塞尔光束在生物医学显微成像技术中的应用[J]. 光子学报，2022，51(8): 0851508.
Chen X L, Wang X Y, Yan T Y, et al. Harnessing the power of Bessel beam for biomedical microscopy[J]. Acta Photonica Sinica，2022，51(8): 0851508.

[22] Durnin J. Exact solutions for nondiffracting beams. I. The scalar theory[J]. Journal of the Optical Society of America A，1987，4(4): 651-654.

[23] Jiang Z P. Truncation of a two-dimensional nondiffracting Cos beam[J]. Journal of the Optical Society of America A，1997，14(7): 1478-1481.

[24] Gutiérrez-Vega J C, Iturbe-Castillo M D, Chávez-Cerda S. Alternative formulation for invariant optical fields: Mathieu beams[J]. Optics Letters，2000，25(20): 1493-1495.

[25] Bandres M A, Gutiérrez-Vega J C, Chávez-Cerda S. Parabolic nondiffracting optical wave fields[J]. Optics Letters，2004，29(1): 44-46.

[26] López-Mariscal C, Bandres M, Gutiérrez-Vega J, et al. Observation of parabolic nondiffracting optical fields[J]. Optics Express，2005，13(7): 2364-2369.

[27] Arrizón V, Chavez-Cerda S, Ruiz U, et al. Periodic and quasi-periodic non-diffracting wave fields generated by superposition of multiple Bessel beams[J]. Optics Express，2007，15(25): 16748-16753.

[28] Vasilyeu R, Dudley A, Khilo N, et al. Generating superpositions of higher order Bessel beams[J]. Optics express，2009，17(26): 23389-23395.

[29] Liu D M, Zhang Y, Hu X P, et al. Flexible tuning of nonlinear non-diffracting array beams using wavelengths and angles[J]. Optics Letters，2020，45(21): 6106-6109.

[30] Kotlyar V V, Kovalev A A, Soifer V A. Asymmetric Bessel modes[J]. Optics Letters，2014，39(8): 2395-2398.

[31] 兰燕平，赖松陶，施逸乐，等. 可调谐的非傍轴自加速光束[J]. 光学学报，2019，39(10): 1026001.
Lan Y P, Lai S T, Shi Y L, et al. Tunable non-paraxial accelerating beams[J]. Acta Optica Sinica，2019，39(10): 1026001.

[32] Lan Y P, Hu F R, Qian Y X. Generation of spirally accelerating optical beams[J]. Optics Letters，2019，44(8): 1968-1971.

Manipulation of Non-Diffracting Beams with Arbitrary Structures Based on Optical Caustics

Lan Yanping[1], Hu Juntao[1], Sun Zhuo[1], Wang Yishu[1], Ye Wenni[1], Qian Yixian[1,2*]

[1]*College of Physics and Electronic Information Engineering, Zhejiang Normal University, Jinhua* 321004, *Zhejiang, China*;

[2]*Key Laboratory of Researching Optical Information Detecting and Display Technology in Zhejiang Province, Jinhua* 321004, *Zhejiang, China*

Abstract

Objective　Structured light beams with controllable intensity distribution have received great interest recently. Many new-type beams exhibit unique physical properties including diffraction-free, self-bending, orbital-angular-momentum-carrying, and abruptly autofocusing. Particularly, non-diffracting beams can retain their intensities and shapes during propagation and have been widely used in laser micromachining, particle manipulation, and microscopic imaging. The first type of non-diffracting beam is the Bessel beam, which was first discovered by Durnin in 1987. It is a wave packet solution expressed as a Bessel function and derived from the Helmholtz equation in a cylindrical coordinate system. Additionally, Bessel beams have a doughnut-shaped intensity distribution and phase singularity at their center and also exhibit many unique optical properties. Most non-diffracting beams are associated with the known, exact solutions of the wave equation and match with special forms of the angular spectrum. It is the angular spectrum that determines the beam propagation dynamics, as well as the intensity profiles. To achieve diverse transverse shapes of non-diffracting beams, a traditional method is to solve the wave equation under different coordinates. For example, the cosine beam, the Mathieu beam, and the Weber beam were obtained by solving a wave equation in a rectangular coordinate system, an elliptic coordinate system, and a parabolic coordinate system, respectively. Later, more non-diffracting beams were constructed by superimposing the basic fundamental non-diffracting beams. Recently, the typical accelerating Airy beam also exhibits unique non-diffracting characteristics as well as self-acceleration and self-healing. However, current methods are limited to producing only a limited non-diffracting structured light beam, which greatly restricts their applications. Consequently, it is imperative to create a greater variety of non-diffracting beams with diverse transverse intensity distributions so that the capabilities of non-diffracting structured light beams can be enhanced. We demonstrate a universal method for designing and generating non-diffracting structured light beams with arbitrary shapes. Such light beams can be tailored by predefining appropriate spectral phases. Unlike conventional approaches, our method overcomes the traditional limitation that these non-diffracting beams are always constructed from wave equation solutions. The ability to produce non-diffracting beams with arbitrary transverse shapes offers potential benefits for manipulating particles along arbitrary transverse trajectories and could inspire new applications in optical micromachining, manipulation, and wavefront control.

Methods　We develop an efficient, simple, and universal optical caustic approach from the perspective of geometric optics. Concretely, our idea is to design a suitable spectral phase to produce a non-diffracting beam with the desired shape. Then, the relationship between the spectral phase and the beam structure is established based on the stationary phase approximation that relies on the cancellation of components due to rapid phase oscillation. Subsequently, the desired non-diffracting beams are generated by imposing the constructed spectral phase on a plane wave. Further, a modified algorithm is developed via spectral phase superposition. In this way, non-diffracting beams with arbitrary structures are generated. Experimentally, the non-diffracting beams with arbitrary shapes can be generated at the focal plane of a Fourier transform lens illuminated by a plane wave, as described in Fig. 4.

Results and Discussions　We break through the traditional constraints of solving the Helmholtz partial differential equation to obtain arbitrary non-diffracting beams. The constructed non-diffracting beams exhibit diverse transverse structures, such as circular and parabolic shapes (Fig. 2), kidney-shaped and 8-shaped (Fig. 3), as well as heart-shaped (Fig. 5). The maximum intensity is always located in the predefined trajectory because the second derivative for the phase part described by Eq. (6) equals zero. The one-to-one correspondence between the transverse beam shape and the spectral phase is established (Eq. (5) and Eq. (7)), and this makes our approach possible to manipulate and generate various non-diffracting beams. Moreover, an improved algorithm is developed to generate non-diffracting beams with arbitrary transverse shapes (Eq. (8)) that can consist of both convex and concave trajectories. The numerical results are consistent with the experimental results (Fig. 6). The non-diffracting property is also discussed, as demonstrated in our numerical and experimental results which exhibit an obvious non-diffracting property. Such non-diffracting beams would also be

advantageous for manipulating particles following arbitrary transverse shapes.

Conclusions   In summary，we develop an effective strategy and a practical technique to achieve non-diffracting beams with an arbitrary transverse intensity distribution. The proposed approach breaks the limitation that the classical non-diffracting beams are always constructed from the solutions of wave equations. The beam shape can be readily customized by the desired spectral phase constructed using optical caustics. The constructed non-diffracting beams with arbitrary shapes greatly enrich the family of structured light beams and would be beneficial to manipulating particles following such transverse shapes. They are likely to provide ideas for new applications in optical micromachining，manipulation，and wavefront control.

Key words   physical optics; non-diffracting beam; optical caustics; phase modulation